0026-895X/08/7305-1502–1512$20.00
MOLECULAR PHARMACOLOGY
Copyright © 2008 The American Society for Pharmacology and Experimental Therapeutics
Mol Pharmacol 73:1502–1512, 2008

Vol. 73, No. 5
44347/3327893
Printed in U.S.A.

Abrogation of Hyperosmotic Impairment of Insulin Signaling by a Novel Class of 1,2-Dithiole-3-thiones through the Inhibition of S6K1 Activation

Eun Ju Bae, Yoon Mee Yang, and Sang Geon Kim

From Innovative Drug Research Center for Metabolic and Inflammatory Diseases, College of Pharmacy and Research Institute of Pharmaceutical Sciences, Seoul National University, Seoul, Korea

Received December 12, 2007; accepted February 5, 2008

ABSTRACT

A previous study from this laboratory showed that oltipraz and synthetic dithiolethiones prevent tumor necrosis factor-α–induced hepatic insulin resistance via AMP-activated protein kinase-dependent p70S6 kinase (S6K) 1 inhibitory pathway. This study investigated whether oltipraz and a novel class of 1,2-dithiole-3-thiones were capable of preventing insulin resistance induced by hyperosmotic stress, thereby enhancing insulin-dependent signals, and, if so, whether the restoration of insulin signal was mediated with the inhibition of S6K1 activity stimulated by hyperosmotic stress. In HepG2 cells, oltipraz treatment inhibited insulin receptor substrate (IRS) 1 serine phosphorylation, a marker of insulin resistance, induced by sorbitol-, mannitol-, or sodium chloride-induced hyperosmotic stress. Consequently, this allowed cells to restore insulin signals, which was evidenced by decrease in the ratio of serine to tyrosine phosphorylations of IRS1 and increase in the phosphorylations of Akt and glycogen synthase kinase (GSK) 3β. Hyperosmotic stress markedly activated S6K1; S6K1 activation was completely abolished by oltipraz pretreatment. An experiment using dominant-negative S6K1 supports the essential role of S6K1 in the hyperosmolarity-stimulated phosphorylation of IRS1. Transfection of constitutive active mutant S6K1 eliminated the protective effect of oltipraz on GSK3β phosphorylation, indicating that oltipraz restores insulin signaling by inhibiting S6K1 activation. A variety of synthetic 1,2-dithiole-3-thione derivatives also inhibited S6K1 activity and insulin resistance induced by hyperosmotic stress in HepG2 cells. The results of this study demonstrate that a novel class of 1,2-dithiole-3-thiones improve insulin sensitivity under the condition of hyperosmotic stress, which results from the inhibition of S6K1 activation.

Insulin is an important regulatory hormone that mediates energy uptake by inhibiting glucose production in liver and by increasing glucose uptake into muscle and fat (Saltiel and Kahn, 2001). Insulin resistance is defined as a profound dysregulation of insulin signaling system and thus represents a state of impaired ability of peripheral tissues to respond to the physiological levels of insulin. Insulin resistance may lead to the development of a variety of metabolic diseases, such as type 2 diabetes, cardiovascular disorders, and liver diseases. In the clinical conditions of diabetes or dehydration, hyperosmotic stress accounts, at least in part, for insulin resistance (Bratusch-Marrain and DeFronzo, 1983; Ennis et al., 1994; Gual et al., 2003a,b). Because inhibition of insulin resistance restores the ability of insulin to suppress hepatic glucose production and to promote glucose uptake in peripheral tissues, pharmaceutical interventions to prevent insulin resistance are of great therapeutic interest.

Binding of insulin to the insulin receptor (IR) initiates signaling cascades by activating its receptor tyrosine kinase. Most signals of IR are transmitted through complexes assembled around insulin receptor substrate (IRS)-1/2, composed of multiple interaction domains and phosphorylation motifs (Myers and White, 1996; Paz et al., 1996). Because IRS1 is

This work was supported by the Korea Science and Engineering Foundation (KOSEF) grant R11-2007-107-01001-0 funded by the Korea government (Ministry of Science and Technology).
Article, publication date, and citation information can be found at http://molpharm.aspetjournals.org.
doi:10.1124/mol.107.044347.

ABBREVIATIONS: IR, insulin receptor; IRS, insulin receptor substrate; mTOR, mammalian target of rapamycin; TNF, tumor necrosis factor; AMPK, AMP-activated protein kinase; S6K, p70S6 kinase; MAPK, mitogen-activated protein kinase; ERK, extracellular signal-regulated kinase; JNK, c-Jun N-terminal kinase; CJ11766, 4-ethyl-5-pyrazin-2-yl-1,2-dithiole-3-thione; CJ11788, 5,6-dihydro-4*H*-cyclopenta-1,2-dithiole-3-thione; CJ11792, 4,5,6,7-tetrahydrobenzo-1,2-dithiole-3-thione; CJ11840, 5-benzo[*b*]thiophene-3-yl-1,2-dithiole-3-thione; CJ11842, 4-methyl-5-phenyl-1,2-dithiole-3-thione; CJ12064, 5-(6-methoxypyrazinyl)-4-methyl-1,2-dithiole-3-thione; CJ12073, 5-(6-ethoxypyrazin-2-yl)-4-methyl-1,2-dithiole-3-thione; FBS, fetal bovine serum; IκB, inhibitor of nuclear factor-κB; ACC, acetyl-CoA carboxylase; DN-S6K1, dominant-negative S6K1; CA-S6K1, constitutively active mutant S6K1; GSK3β, glycogen synthase kinase 3β.

centrally located within the insulin-signaling pathway, defects of IRS1 function significantly impair downstream responses of insulin receptor (Yamauchi et al., 1996). In particular, IRS1 serine phosphorylation leads to decreases in its tyrosine phosphorylation (Hotamisligil et al., 1996) and increase in the proteasome-mediated degradation (Sun et al., 1999). Hence, serine phosphorylations and/or degradation of IRS1 play a key role in insulin resistance. Other studies indicated that insulin resistance by hyperosmolarity is also mediated by IRS1 dysfunction (Gual et al., 2003a).

Ligand-activated IR and tyrosine-phosphorylated IRS1 relay signal transmission to the phosphoinositide 3-kinase–Akt pathway, and activation of this pathway then enhances mammalian target of rapamycin (mTOR)-p70S6 kinase (S6K) 1 activity. Studies showed that insulin resistance induced by certain pathophysiological situations (e.g., hyperinsulinemia and obesity) or excess nutrient availability is linked to marked increases in S6K1 activity (Um et al., 2004; Tremblay et al., 2005). A S6K1 knockout experiment strengthened the physiological importance of the inhibitory regulation of mTOR-S6K1 to insulin signaling (Um et al., 2004), which suggests the mTOR-S6K1 pathway as an attractive therapeutic target for insulin resistance.

In our previous study, we found that oltipraz and novel dithiolethiones prevent TNFα-induced hepatic insulin resistance through AMP-activated protein kinase (AMPK)-dependent S6K1 inhibition (Bae et al., 2007). Hyperosmotic stress has been shown to activate the mTOR pathway (Gual et al., 2003a), which causes insulin resistance. However, the kinase downstream of mTOR leading to hyperosmotic insulin resistance has not been clarified yet. It seemed to us that the activation of S6K1 is highly likely to be responsible for insulin resistance induced by hyperosmotic stress. Hyperosmolarity also activates AMPK via a mechanism that remains unclear (Hayashi et al., 1998; Fryer et al., 2000; Hayashi et al., 2000), which occurs presumably as an adaptive response to toxic external stress, as indicated by cell shrinkage with decrement of cell water volume and the dissipation of mitochondrial transmembrane potential (Fumarola et al., 2005). Therefore, the activation of AMPK by hyperosmotic stress might not be a beneficial signaling pathway for insulin sensitivity. In view of the potential important role of mTOR-S6K1 pathway in hyperosmotic insulin resistance, we examined whether oltipraz and newly synthesized derivatives were capable of preventing insulin resistance induced by hyperosmotic stress, thereby enhancing insulin dependent signals and, if so, whether the restoration of insulin signal was mediated with the inhibition of S6K1 activity stimulated by hyperosmotic stress. Here, we report identification of the compounds comprising 1,2-dithiole-3-thione as a pharmacophore that prevent insulin resistance induced by hyperosmotic stresses as a consequence of the inhibition of S6K1 activation.

Materials and Methods

Materials

Oltipraz was provided from CJ Corporation (Seoul, Korea). Sorbitol was purchased from Sigma Chemicals (St. Louis, MO). [γ-^{32}P]ATP (3000 mCi/mmol) was supplied from PerkinElmer Life and Analytical Sciences (Waltham, MA). Antibodies directed against IRS1, IRβ, S6K1, and inhibitor of nuclear factor-κB (IκB) α were obtained from Santa Cruz Biotechnology (Santa Cruz, CA). Anti-phosphotyrosine (4G10) and anti-p-Ser^{312}-IRS1 (Ser^{307} in rodent form) antibodies were purchased from Millipore (Billerica, MA). Antibodies specific for S6, GSK3β, ERK, JNK, p38 mitogen-activated protein kinase (MAPK), β-actin and phospho-specific antibodies directed against p-ACC(Ser^{79}), p-S6K1(Thr^{389}), p-S6K1(Thr^{421}/Ser^{424}), p-S6(Ser$^{235/236}$), p-S6(Ser$^{240/244}$), p-4E-BP1(Thr$^{37/41}$), p-Akt(Ser^{473}), p-GSK3β(Ser^{9}), p-ERK, p-JNK, and p-p38 MAPK were supplied from Cell Signaling Technology (Danvers, MA). Horseradish peroxidase-conjugated goat anti-rabbit and goat anti-mouse IgGs were provided from Zymed Laboratories (South San Francisco, CA).

Chemical Synthesis of 1,2-Dithiol-3-thione Analogs

1,2-Dithiol-3-thione analogs were synthesized at CJ Central Laboratories (Ichon City, Korea) according to the methods described by Curphey (2002), as described previously (Bae et al., 2007).

4-Methyl-5-(2-pyrazinyl)-1,2-dithiol-3-thione (Oltipraz). Methyl 2-methyl-3-(pyrazin-2-yl)-3-oxopropionate (40 g, 206 mmol) dissolved in 100 ml of toluene was added drop-wise to the mixture of 300 ml of toluene, 350 ml of xylene, and 48 g of phosphorus pentasulfide. Oltipraz crystal obtained from chemical reaction of the mixture was filtered, washed, and vacuum-dried (6.37 g, 13.6% yield, >99.5% purity). NMR (400 MHz, $CDCl_3$): 2.51(s, 3H), 8.70(d, 1H), 8.80(d, 1H), 9.21(s, 1H).

4-Ethyl-5-pyrazin-2-yl-1,2-dithiole-3-thione (CJ11766). Phosphorus pentasulfide (3.36 g, 7.56 mmol) suspended in 40 ml each of toluene and xylene was heated to boiling point, and methyl 2-ethyl-3-oxo-3-pyrazin-2-yl-propionate (1.5 g, 7.20 mmol) was added to the solution. After reflux for 4 h, the reaction mixture was cooled to ambient temperature and filtered through Celite (Sigma). Water (100 ml) and methanol (20 ml) were added to the filtrate, and the bilayer solution was neutralized with 28% NH_4OH. Separation of organic layer was followed by washing with brine and drying over anhydrous $MgSO_4$. Evaporation of filtrate and purification by flash chromatography on silica gel offered 0.20 g of 4-ethyl-5-pyrazin-2-yl-1,2-dithiole-3-thione (11.5% yield). NMR (400 MHz, $CDCl_3$): 1.20(t, 3H), 2.90(q, 2H), 8.75(s, 2H), 8.90(s, 1H).

5,6-Dihydro-4*H*-cyclopenta-1,2-dithiole-3-thione (CJ11788). Phosphorus pentasulfide (4.68 g) suspended in 50 ml each of toluene and xylene was heated to boiling point, and 3 ml of 2-oxo-cyclopentanecarboxylic acid ethylester was added to the solution. After reflux for 5 h, the reaction mixture was cooled to ambient temperature, and filtered through Celite. Water (100 ml) and methanol (20 ml) were added to the filtrate, and the bilayer solution was neutralized with 28% NH_4OH. The organic layer was separated, followed by washing with brine and drying over anhydrous $MgSO_4$. Evaporation of filtrate and purification by flash chromatography on silica gel (ethyl acetate/*n*-hexane = 1:30) afforded 0.7 g of 5,6-dihydro-4*H*-cyclopenta-1,2-dithiole-3-thione (20% yield). NMR (400 MHz, $CDCl_3$): 2.65–2.80(m, 4H), 2.95–3.00(m, 2H).

4,5,6,7-Tetrahydrobenzo-1,2-dithiole-3-thione (CJ11792). To a mixture of 3 ml each of tetrahydrofuran and dimethylformamide was added potassium *t*-butoxide (460 mg) under argon gas. At room temperature, cyclohexanone (0.17 ml) in 1 ml tetrahydrofuran was injected, and the mixture was stirred for 15 min. Addition of 0.11 ml carbon disulfide was followed by stirring for 30 min, injection of 0.52 ml of hexamethyldisilathian and then stirring for 1 h at room temperature. After cooling to 3°C, 1.80 mmol of hexachloroethane in 2 ml tetrahydrofuran was added, the reaction solution was stirred for 30 min. Quenching with 2 ml of methanol and evaporation of volatile materials gave sticky red oil, which was purified by flash chromatography on silica gel (ethyl acetate/*n*-hexane = 1:30). Then, 77 mg of 4,5,6,7-tetrahydrobenzo-1,2-dithiole-3-thione was obtained as a red solid (25% yield). NMR (400 MHz, $CDCl_3$): 1.75–7.90(m, 4H), 2.55–2.60(m, 2H), 2.80–2.85(m, 2H).

5-Benzo[*b*]thiophene-3-yl-1,2-dithiole-3-thione (CJ11840). To a solution of potassium *t*-butoxide (1.07 g) in 20 ml of tetrahydrofuran was injected 800 mg of 1-benzo[*b*]thiophen-3-yl-ethanone dissolved in 5

ml of tetrahydrofuran. After stirring for 15 min, 0.3 ml of carbon disulfide was added, and the mixture was stirred for 30 min followed by addition of 2.83 mg methyl iodide and stirring at room temperature to complete reaction. Work-up was performed as a sequence of dilution with 50 ml of methylene chloride, neutralization with saturated NH_4Cl solution, and separation of organic layer. After concentration, purification by flash chromatography on silica gel (ethyl acetate/*n*-hexane = 1:10) gave 700 mg of yellow solid as a bis-methylsulfide adduct. Dissolution of this solid in 15 ml each of toluene and xylene, followed by addition of 0.58 g of phosphorus pentasulfide, made a suspension to be refluxed for 3 h. The reaction mixture was cooled to ambient temperature, and filtered through Celite. Water (50 ml) was added to the filtrate, and the bilayer solution was neutralized with 28% NH_4OH. Separation of organic layer was followed by washing with brine and drying over anhydrous $MgSO_4$. Evaporation of filtrate and purification by flash chromatography on silica gel (ethyl acetate/*n*-hexane = 1:30) offered 185 mg of 5,6-dihydro-4*H*-cyclopenta-1,2-dithiole-3-thione (15.3% yield). NMR (400 MHz, $CDCl_3$): 7.45–7.55(m, 3H), 7.95(d, 1H), 8.00(s, 1H), 8.10(d, 1H).

4-Methyl-5-phenyl-1,2-dithiole-3-thione (CJ11842). To a mixture of 4 ml of tetrahydrofuran and 2 ml of *N*,*N*′-dimethylpropyleneurea was added 407 mg of potassium *t*-butoxide under argon gas. At room temperature, 0.22 ml of 1-phenyl-propan-1-one was injected, and the mixture was stirred for 15 min. Addition of 0.11 ml of carbon disulfide was followed by stirring for 15 min, injection of 0.52 ml of hexamethyldisilathian, and then stirring for 15 min at room temperature. After cooling to 3°C, 391 mg of hexachloroethane in 2 ml of tetrahydrofuran was added, and the reaction solution was stirred for 30 min. Quenching with 2 ml of methanol and evaporation of volatile materials gave sticky red oil, which was purified by flash chromatography on silica gel (ethyl acetate/*n*-hexane = 1:60), and then 78 mg of 4-methyl-5-phenyl-1,2-dithiole-3-thione was obtained as a red solid (21% yield). NMR (400 MHz, $CDCl_3$): 2.25(s, 3H), 7.55–7.60(m, 5H).

5-(6-Methoxypyrazinyl)-4-methyl-1,2-dithiole-3-thione (CJ12064). 5-(6-Chloro-pyrazinyl)-4-methyl-1,2-dithiole-3-thione (200 mg) and 0.32 g of potassium carbonate were dissolved in 10 ml methanol, and the mixture was refluxed for 2 h. Evaporation of solvent was followed by the addition of saturated NH_4Cl aqueous solution and the extraction with methylene chloride. After concentration, titration with *n*-hexane yielded 140 mg of a red solid 5-(6-methoxypyrzin-2-yl)-4-methyl-1,2-dithiole-3-thione (71.2% yield). NMR (400 MHz, $CDCl_3$): 2.55(s, 3H), 4.40(s, 3H), 8.35(s, 1H), 8.55(s, 1H).

5-(6-Ethoxypyrazin-2-yl)-4-methyl-1,2-dithiole-3-thione (CJ12073). 5-(6-Chloro-pyrazin-2-yl)-4-methyl-1,2-dithiole-3-thione (200 mg, 0.77 mmol) and 0.32 g of potassium carbonate were dissolved in 10 ml of ethanol, and the mixture was refluxed for 2 h. Evaporation of solvent was followed by the addition of saturated NH_4Cl aqueous solution and the extraction with methylene chloride. After concentration, titration with *n*-hexane yielded red solid 140 mg of 5-(6-ethoxypyrazin-2-yl)-4-methyl-1,2-dithiole-3-thione (67.5% yield). NMR (400 MHz, $CDCl_3$): 1.45(t,J = 7Hz,3H), 2.55(s,3H), 4.45(q,J = 7Hz,2H), 8.35(s,1H), 8.55(s,1H).

Cell Culture and Drug Treatments

HepG2 hepatocyte, C2C12 myoblast, and 3T3-L1 preadipocyte cell lines were purchased from American Type Culture Collection (Manassas, VA). The cells were maintained in Dulbecco's modified Eagle's medium containing 10% fetal bovine serum (FBS), 50 units/ml penicillin, and 50 μg/ml streptomycin (complete medium). C2C12 cells were differentiated to myotubes by incubating in Dulbecco's modified Eagle's medium containing 2% FBS for 6 to 8 days. 3T3-L1 preadipocytes were differentiated to adipocytes, as described previously (Bae and Kim, 2005). In brief, 2 day-postconfluent preadipocytes were treated with 0.5 mM isobutyl-1-methylxanthine, 1 μM dexamethasone, and 1 μg/ml insulin for 2 days. The cells were then incubated in the complete medium containing insulin for 2 additional days and thereafter exposed to the complete medium without insulin for 2 to 4 days. To assess IRS1 serine phosphorylation, the cells were deprived of serum for 24 h, pretreated with oltipraz for 1 h, and subsequently exposed to 600 mM sorbitol, 600 mM mannitol, or 150 mM NaCl for the time periods (indicated in the figure legends) in the continuing presence of oltipraz. To set an insulin resistance model, the cells were incubated with sorbitol for 50 min and then treated with 10 nM insulin for 10 min. Cell lysates were prepared according to methods published previously (Kang et al., 2003). In brief, cells were centrifuged at 3000*g* for 3 min and allowed to swell after the addition of lysis buffer. The samples were centrifuged at 10,000*g* for 10 min to obtain lysates and stored −70°C until use.

Immunoblot Analysis

Immunoblot analysis were performed according to the previously published procedures. Proteins of interest in lysates were resolved using 6, 9, or 12% gels and developed using ECL chemiluminescence system (GE Healthcare, Chalfont St. Giles, Buckinghamshire, UK).

Immunoprecipitation

To assess tyrosine-phosphorylated IRβ or IRS1, cell lysates (250 μg each) were incubated with anti-IRβ or anti-IRS1 antibody overnight at 4°C. The antigen-antibody complex was immunoprecipitated after incubation for 2 h at 4°C with protein G-agarose. Immune complexes were solubilized in 2× Laemmli buffer. Protein samples were resolved and immunoblotted with anti-phosphotyrosine antibody.

Plasmid Transfection

The S6K1 expression constructs PRK5 myc-tagged E2BQ (dominant-negative, DN-S6K1) and D3E (constitutively active, CA-S6K1) were supplied from Dr. J. Han (Sungkyunkwan University, Suwon, Korea), originally provided by Dr. G. Thomas (Friedrich Miescher Institut, Basel, Switzerland) (Pearson et al., 1995; Jefferies et al., 1997). HepG2 cells (5×10^5 cells/well) were replated in six-well plates overnight, serum-starved for 6 h, and transfected with DN-S6K1 or CA-S6K1 (1 μg) in the presence of Lipofectamine Reagent (Invitrogen, Carlsbad, CA). The transfected cells were incubated in Eagle's minimum essential medium containing 1% FBS for 24 h and exposed to sorbitol in the presence or absence of oltipraz.

S6K1 Activity

S6K1 activities were determined by immunocomplex kinase assays. S6K1 was immunoprecipitated in lysates of HepG2 cells treated with 30 μM oltipraz or other dithiolethiones for 1 h, and subjected to kinase reactions. To assess the direct in vitro effects of oltipraz, S6K1 immunoprecipitates obtained from the cell lysates were incubated with oltipraz in a kinase reaction mixture. Kinase reactions were initiated by adding S6 RSK substrate peptide (5 μg per assay; Santa Cruz Biotechnology) and 1 μCi of [γ-^{32}P]ATP (3000 mCi/mmol) to 20 μl of kinase buffer containing 25 mM Tris-HCl, pH 7.4, 10 mM $MgCl_2$, 25 mM β-glycerophosphate, 1 mM Na_3VO_4, 2 mM dithiothreitol, 1 mM phenylmethylsulfonyl fluoride, 1 μg/ml leupeptin, and 200 μM ATP, and continued for 20 min at 30°C. After brief centrifugation, the supernatants of reaction mixture were spotted onto p81 Whatman phosphocellulose paper (Whatman Bioscience, Clifton, NJ). The paper was washed with 0.8% phosphoric acid three times for 15 min each and subsequently with 90% ethanol for 5 min. The membrane was dried and the radioactivity of phosphorylated substrate was measured using a β-counter (PerkinElmer Life and Analytical Sciences, Waltham, MA).

Glucose Uptake

Differentiated myotubes and adipocytes were incubated with each agent of interest in the presence or absence of 600 mM sorbitol for 50 min. After the change of culture medium with phosphate-buffered saline, cells were treated with 100 nM insulin for 10 min, and glucose uptake was determined by 2-deoxy-D-[2,6-^{3}H]glucose incorporation into the cells for 20 min. The reaction was terminated by adding

ice-cold phosphate-buffered saline. After washing three times, the cells were dissolved in 0.5 N NaOH containing 0.1% SDS. Radioactivity was measured using a scintillation counter. Specific uptake was assessed by subtracting nonspecific uptake, which was measured by incubating the cells with 20 μM cytochalasin B. Values were normalized by protein amounts.

Data Analysis

Scanning densitometry was performed with Image Scan and Analysis System (Alpha Innotech, San Leandro, CA). Student's t test was used to assess significant differences between control and treatment group and one-way analysis of variance procedures among treatment groups. The criterion for statistical significance was set at $p < 0.05$ or 0.01.

Results

Inhibition of Hyperosmotic Stress-Induced IRS1 Serine Phosphorylation by Oltipraz. Human IRS1 Ser^{312} phosphorylation, corresponding to Ser^{307} in the rodent form, is a representative molecular marker of insulin resistance (Aguirre et al., 2000, 2002). Because insulin resistance induced by hyperosmolarity involves the IRS1 serine phosphorylations (Gual et al., 2003a), we first investigated the effect of oltipraz on hyperosmotic stress-induced IRS1 Ser^{312} phosphorylation in HepG2 cells. A time-course study showed that IRS1 serine phosphorylation began to increase as early as 10 min after 600 mM sorbitol treatment, which maximally increased at 1 h and maintained for at least 3 h (Fig. 1A). Pretreatment of the cells with oltipraz inhibited sorbitol-induced IRS1 Ser^{312} phosphorylation at the time points examined. The dose-response study indicated that pretreatment with 30 to 60 μM oltipraz effectively blocked the IRS1 serine phosphorylation (Fig. 1B). Because 30 μM oltipraz was highly active, we chose the concentration in the subsequent experiments.

Studies have shown that 300 to 600 mM mannitol or 150 mM sodium chloride also induces hyperosmotic stress (Kültz et al., 1997; Galvez et al., 2003). Oltipraz similarly inhibited IRS1 serine phosphorylation induced by hyperosmolar mannitol or sodium chloride (Fig. 1C). These results provide evidence that oltipraz inhibited IRS1 Ser^{312} phosphorylation against hyperosmotic stress.

Oltipraz Protection of Insulin Signaling. Next, we measured insulin signaling in the cells treated with sorbitol or oltipraz+sorbitol. Exposure of the cells to insulin caused increases in IRβ/IRS1 tyrosine phosphorylations, and Akt serine phosphorylation (Fig. 2A, upper). Concomitant sorbitol treatment unchanged the total or tyrosine-phosphorylated IRβ levels in insulin-treated cells, whereas the levels of IRS1 tyrosine phosphorylation and Akt phosphorylations were both decreased. We also found that IRS1 serine phosphorylation was reciprocal to its tyrosine phosphorylation. These data suggest that hyperosmotic stress does not impair the tyrosine kinase activity of insulin receptor, which is consistent with the previous reports (Chen et al., 1999; Gual et al., 2003a). Oltipraz treatment before sorbitol exposure allowed the cells to recover insulin-dependent IRS1 tyrosine phosphorylation with a commensurate decrease in the serine phosphorylation. Therefore, the ratios of IRS1 serine to tyrosine phosphorylations significantly decreased after oltipraz pretreatment (Fig. 2A, lower). Accordingly, oltipraz pre-

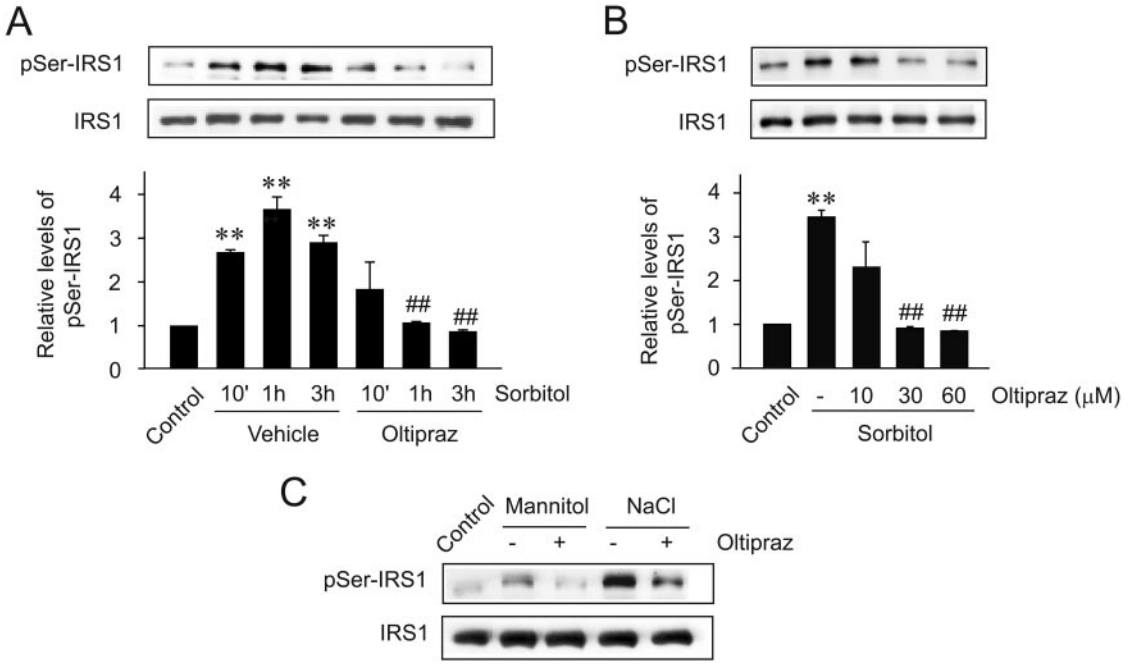

Fig. 1. Oltipraz inhibits IRS1 Ser^{312} phosphorylation of induced by hyperosmotic stress. A, the time responses of hyperosmotic stress-dependent IRS1 Ser^{312} phosphorylation. Immunoblot analysis was performed in lysates of HepG2 cells treated with 30 μM oltipraz for 1 h and subsequently exposed to 600 mM sorbitol for the indicated time period. The relative levels of IRS1 Ser^{312} phosphorylation were assessed by scanning densitometry of the immunoblots. Data represent mean ± S.E. with at least 3 separate experiments (**, $p < 0.01$, significant compared with vehicle control; significant compared with respective sorbitol treatment; ##, $p < 0.01$; control level = 1). B, the dose-responses of oltipraz treatment on sorbitol-induced IRS1 Ser^{312} phosphorylation. The cells were treated with 10 to 60 μM oltipraz for 1 h and subsequently exposed to 600 mM sorbitol for 1 h. The values represent mean ± S.E. with three separate experiments (**, $p < 0.01$, significant compared with vehicle control; ##, $p < 0.01$, significant compared with sorbitol alone). C, oltipraz's inhibition of IRS1 Ser^{312} phosphorylation induced by hyperosmolar mannitol or sodium chloride. The cells were treated with 30 μM oltipraz for 1 h and then exposed to 600 mM mannitol or 150 mM sodium chloride for 1 h in the continuing presence of oltipraz.

treatment enhanced insulin-dependent Akt phosphorylation against hyperosmotic stress.

Because sorbitol impairs the activity of Akt responsible for the phosphorylation of downstream GSK3β, insulin-stimulated GSK3β phosphorylations became defective after sorbitol treatment. Oltipraz treatment allowed the cells to restore insulin-dependent GSK3β phosphorylation in a concentration-dependent manner (Fig. 2B, top and bottom).

The Effects of Oltipraz on Hyperosmotic Stress-Induced Alterations of Cell Signaling. Because IRS1 Ser^{312} phosphorylation is catalyzed by multiple serine/threonine kinases, including S6K1, JNK, ERK, and IκB kinase complex (Aguirre et al., 2000, 2002; Engelman et al., 2000; Gao et al., 2002; Um et al., 2004), we next determined the activation statuses of the kinase signals in the cells treated with sorbitol or oltipraz + sorbitol. S6K1 immunocomplex kinase assays revealed that oltipraz dose-dependently inhibited the basal S6K1 kinase activity. Oltipraz at 3 μM began to inhibit the cellular S6K1 kinase activity, and the inhibition of S6K1 activity by 30 μM oltipraz was comparable with that caused by rapamycin, an mTOR inhibitor (Fig. 3A, top). Incubation of S6K1 immunoprecipitate, which was prepared from untreated HepG2 cell lysates, with oltipraz in vitro resulted in no change in S6K1 activity (data not shown), confirming our previous observation that oltipraz does not directly inhibit S6K1. Likewise, oltipraz notably decreased the basal S6 phosphorylation, which represents cellular S6K1 activity (Fig. 3A, bottom). Next, we determined the effect of oltipraz on sorbitol-induced S6K1 activation. Treatment of HepG2 cells with sorbitol for 10 min~1 h caused S6K1 activation, the extent of which was similar to that induced by insulin (10 nM, 30 min) (Fig. 3B, top). Sorbitol-induced S6K1 activation was significantly inhibited by simultaneous oltipraz treatment throughout the time points examined. Consistent with this result, S6 phosphorylation markedly increased by sorbitol treatment was almost completely inhibited by oltipraz as a function of time (Fig. 3B, bottom).

Further immunoblot analysis showed that hyperosmotic sorbitol promoted S6K1 phosphorylations at Thr^{389} or Thr^{421}/Ser^{424} (Fig. 3C). Concomitant oltipraz treatment essentially eliminated phosphorylations of S6K1 induced by hyperosmotic stress. 4E-BP1 phosphorylation, which is also catalyzed by mTOR, was also prevented by oltipraz treatment. These results indicate that oltipraz affects the mTOR pathway.

Previous observations indicated that hyperosmotic stress activates JNK, ERK, and p38 MAPK (Galcheva-Gargova et al., 1994; Han et al., 1994; Kayali et al., 2000), which prompted us to determine the effect of oltipraz on these kinases. Hyperosmotic sorbitol treatment increased the phosphorylations of JNK, ERK, and p38 MAPK, which were unaffected by oltipraz treatment (Fig. 3D). Hyperosmotic

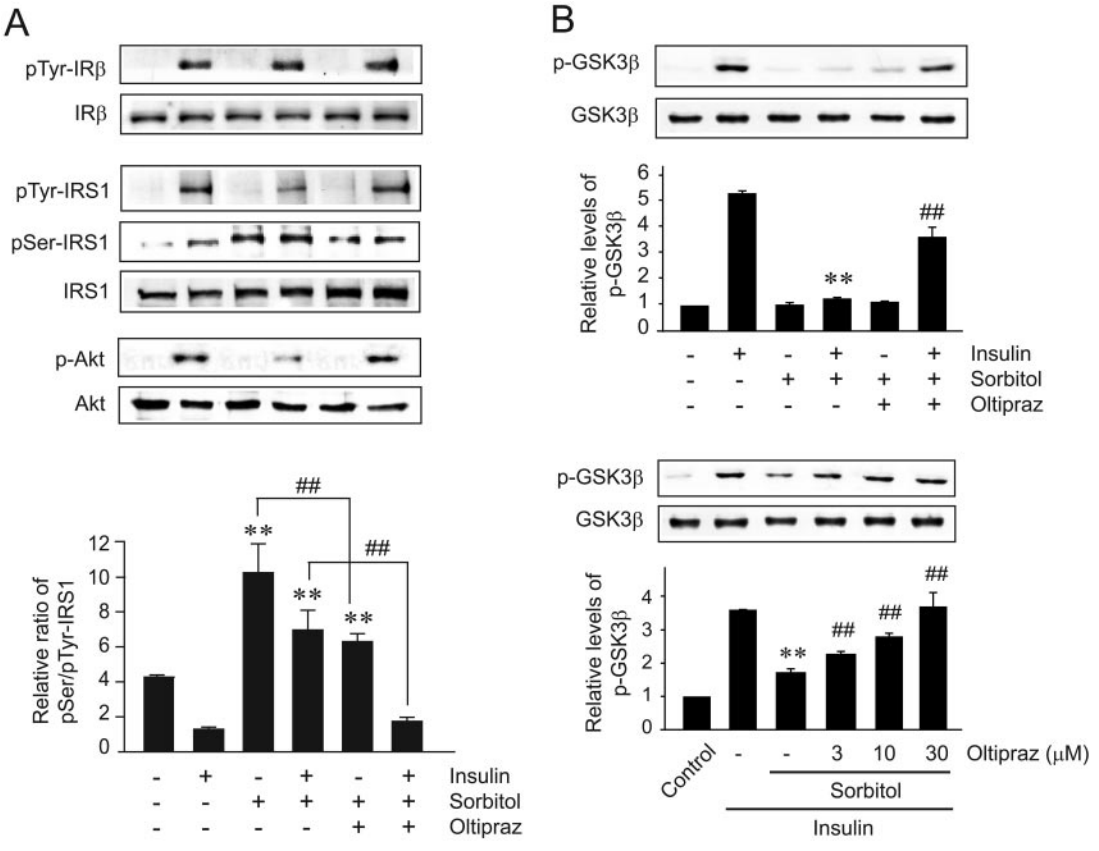

Fig. 2. Oltipraz protects insulin signals against hyperosmotic stress. A, phosphorylations of IRβ, IRS1, and Akt. HepG2 cells were treated with 30 μM oltipraz for 1 h, exposed to 600 mM sorbitol for 50 min, and then continuously incubated with 10 nM insulin for 10 min. IRβ or IRS1 immunoprecipitates were immunoblotted with anti-phosphotyrosine antibody. IRS1 Ser^{312} phosphorylations or Akt Ser^{473} phosphorylations were measured in cell lysates. The bar graphs represent the relative ratios of serine- to tyrosine-phosphorylations of IRS1. Data represent mean ± S.E. with at least three separate experiments (**, $p < 0.01$, significant compared with insulin; ##, $p < 0.01$, significant compared with sorbitol or sorbitol + insulin). B, GSK3β Ser phosphorylations. The relative levels of p-GSK3β Ser^{9} in cells treated, as indicated, were depicted in the bar graph. Data represent mean ± S.E. with at least three separate experiments (**, $p < 0.01$, significant compared with insulin; ##, $p < 0.01$, significant compared with sorbitol + insulin).

stress strongly activates nuclear factor-κB through proteasomal degradation of IκBα (Eisner et al., 2006). Oltipraz did not change IκBα degradation, which is consistent with previous observations (Bae et al., 2007). As an effort to assess the effects of oltipraz on AMPK that is also activated by hyperosmotic stress, we determined the phosphorylations of ACC, an AMPK substrate. Sorbitol increased ACC phosphorylation, which was not abolished by oltipraz treatment. All of these results indicate that oltipraz selectively inhibited the activation of S6K1 among the cellular kinases examined.

The Role of S6K1 Inhibition in Hyperosmotic Stress-Induced IRS1 Serine Phosphorylation. It has been shown that S6K1 activation causes phosphorylation of IRS1 at multiple serine residues (e.g., Ser^{312} and Ser$^{636/639}$ in human; Ser^{302}, Ser^{307}, and Ser$^{632/635}$ in rodents)(Harrington et al., 2004; Um et al., 2004; Tremblay et al., 2005). Having identified oltipraz inhibition of S6K1 activation, we next examined the possible role of S6K1 inhibition in sorbitol-induced IRS1 Ser^{312} phosphorylation. Exposure of HepG2 cells to sorbitol for 1 h resulted in IRS1 serine phosphorylation, which was repressed by dominant-negative mutant S6K1 (DN-S6K1) (Fig. 4A). Inhibition of S6K1 phosphorylation after DN-S6K1 transfection verified transfection efficiency. Rapamycin also inhibited IRS1 serine phosphorylation induced by sorbitol (Fig. 4B). These results support the concept that the inhibition of S6K1 activation leads to

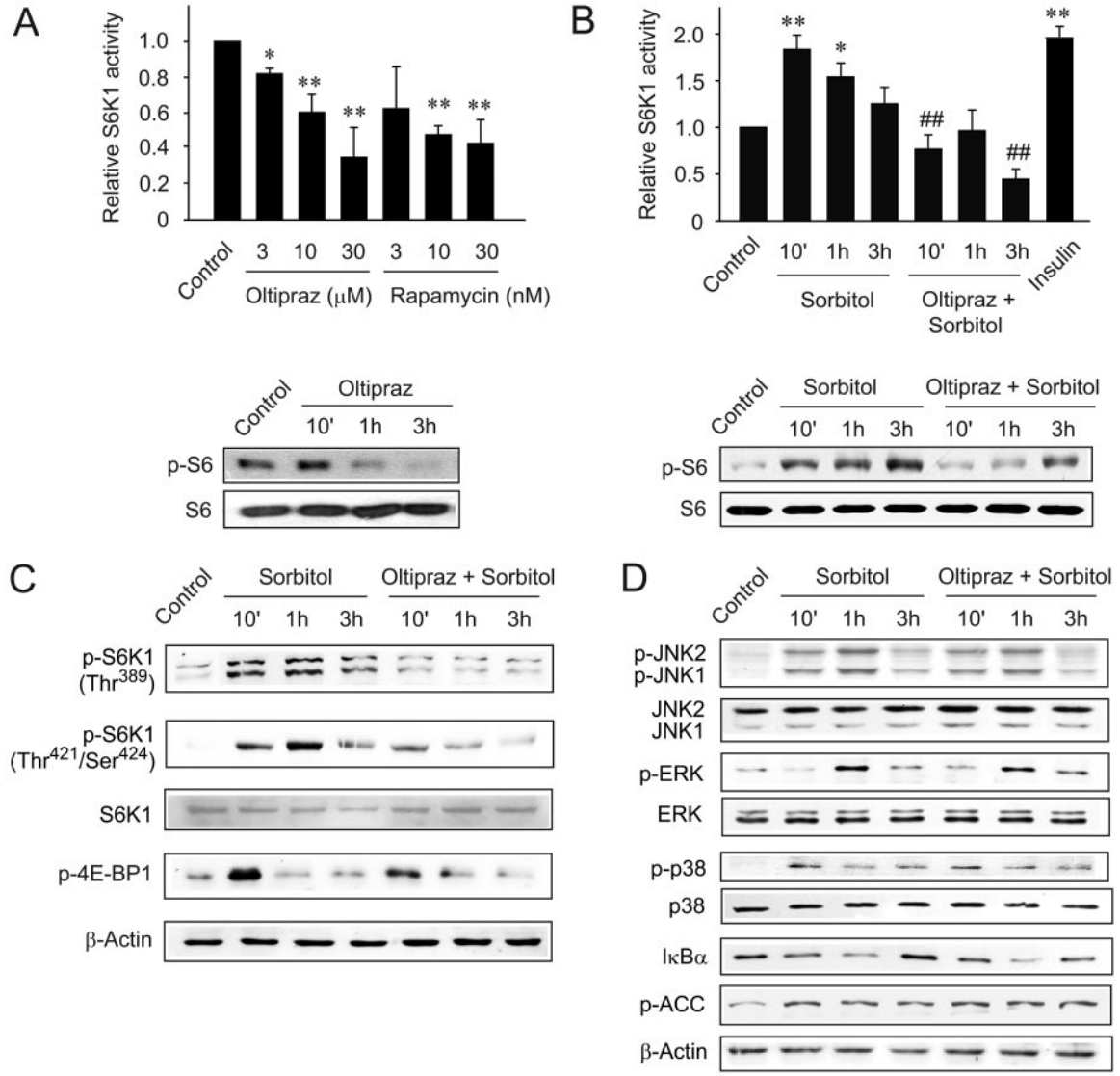

Fig. 3. Oltipraz inhibits the basal and hyperosmolar activation of S6K1. A, inhibition of S6K1 activity by oltipraz. HepG2 cells were treated with 3 to 30 μM oltipraz or 3 to 10 nM rapamycin for 1 h. S6K1 kinase activities in cell lysates were determined toward S6 RSK substrate peptide by immunocomplex kinase assays. Data represent mean ± S.E. with at least three separate experiments (significant compared with vehicle-treated control, *, $p < 0.05$; **, $p < 0.01$; control level = 1). Time responses of S6 phosphorylations after oltipraz treatment (bottom). HepG2 cells were incubated with 30 μM oltipraz for the indicated time periods, and the cell lysates were subjected to immunoblotting with antibody specific for p-S6 (Ser$^{235/236}$). B, inhibition of sorbitol-induced S6K1 activity by oltipraz. HepG2 cells were treated with 600 mM sorbitol for the indicated time period with or without 30 μM oltipraz pretreatment for 1 h. S6K1 activation by insulin (10 nM, 30 min) was included as a positive control. Data represent mean ± S.E. with at least three separate experiments (*, $p < 0.05$, **, $p < 0.01$, significant compared with vehicle-treated control; ##, $p < 0.01$, significant compared with respective sorbitol treatment; control level = 1). The phosphorylations of S6 were determined in HepG2 cells that had been exposed to 600 mM sorbitol with or without oltipraz pretreatment for 1 h (bottom). C, inhibition of sorbitol-induced of S6K1 or 4E-BP1 phosphorylations by oltipraz. Immunoblot analyses were conducted in lysates of HepG2 cells treated as described in B. D, the effects of oltipraz treatment on sorbitol-induced JNK, ERK, p38 MAPK, ACC phosphorylations, and degradation of IκBα. Results were confirmed by repeated experiments.

the inhibition of hyperosmotic stress-induced IRS1 serine phosphorylation.

Abrogation by Constitutively Active Mutant S6K1 of Oltipraz's Protection of Insulin-Induced GSK3β Phosphorylation. To verify the functional role of S6K1 inhibition in oltipraz's restoration of insulin sensitivity under hyperosmotic stress condition, we further determined the effect of constitutively active mutant S6K1 (CA-S6K1) on GSK3β phosphorylation. In this experiment, HepG2 cells were transfected with the plasmid encoding CA-S6K1 and subsequently treated with sorbitol in combination with insulin. CA-S6K1 transfection virtually eliminated the protective effect of oltipraz on insulin-dependent GSK3β phosphorylation (Fig. 5), which indicates that the protection of insulin responses by oltipraz against hyperosmolar sorbitol is mediated with inhibition of S6K1 activation. Immunoblots for c-Myc and phosphorylated S6 confirmed transfection efficiency. Our findings concerning the inhibition of IRS1 serine phosphorylation and of S6K1 activation proved the pharmacologic effect of oltipraz on hyperosmotic stress-induced insulin resistance.

The Effect of Oltipraz on ACC Phosphorylation in Cells Treated with TNFα. In an additional experiment, TNFα was compared with hyperosmolar sorbitol for the effect of oltipraz on ACC phosphorylation in HepG2 cells. Oltipraz treatment allowed the cells to restore AMPK activity inhibited by TNFα (Fig. 6A). The increase in ACC phosphorylation by oltipraz was weaker than that caused by sorbitol. We also observed that oltipraz treatment did not further increase ACC phosphorylation in the cells treated with hyperosmolar sorbitol. These results suggest that S6K1 activation by TNFα was associated with AMPK activity and that the pathway responsible for mTOR-S6K1 activation by hyperosmolarity may differ from that by TNFα. The effects of oltipraz against hyperosmolarity and TNFα challenge were summarized in Fig. 6B.

The Effects of 1,2-Dithiole-3-thione Derivatives on Cellular S6K1 Activity and GSK3β Phosphorylations. Because our results indicated that oltipraz improves insulin actions under the conditions of hyperosmotic stress through the inhibition of S6K1 activation, we tested the effects of 1,2-dithiole-3-thione derivatives to find additional new compounds capable of inhibiting S6K1 activation. Among the synthetic 1,2-dithiole-3-thione derivatives (Fig. 7A), we identified several compounds that inhibited the basal S6K1 activity and would thus be expected to inhibit hyperosmotic stress-induced insulin resistance. Figure 7B shows that CJ11766 and CJ11788, CJ11792, CJ11842, or CJ12064 significantly inhibited the activity of S6K1. In addition, most of the compounds were capable of suppressing sorbitol-induced IRS1 serine phosphorylation (data not shown). To correlate the inhibition of cellular S6K1 activity by these compounds with the recovery of insulin action, we monitored insulin-dependent GSK3β phosphorylation in the cells. As expected, synthetic 1,2-dithiole-3-thione derivatives capable of inhibiting S6K1 activity allowed the cells to recover the insulin signaling (Fig. 7C).

The Effects of Oltipraz and Other 1,2-Dithiole-3-Thione Derivatives on Cell Signaling and Glucose Uptake in C2C12 Myotubes and 3T3-L1 Adipocytes. Next, we assessed the effects of oltipraz on AMPK and S6K1 in other types of cells. In differentiated C2C12 myotubes, olti-

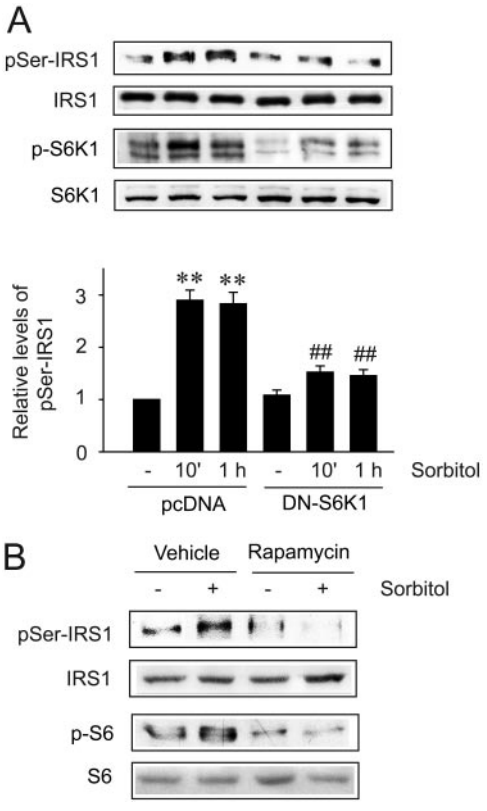

Fig. 4. S6K1 induces IRS Ser^{312} phosphorylation in response to hyperosmotic stress. A, reversal of sorbitol-induced IRS Ser phosphorylation by DN-S6K1. HepG2 cells transfected with pcDNA or a plasmid encoding DN-S6K1 (1 μg) were treated with 600 mM sorbitol for the indicated time period. Data represent mean ± S.E. with at least three separate experiments (**, $p < 0.01$, significant compared with vehicle-treated control; ##, $p < 0.01$, significant compared with respective sorbitol treatment). B, the effect of rapamycin, an mTOR inhibitor, on sorbitol-induced IRS1- Ser^{312} phosphorylation. HepG2 cells were treated with 10 nM rapamycin for 1 h and exposed to 600 mM sorbitol for 1 h in the continuing presence of rapamycin.

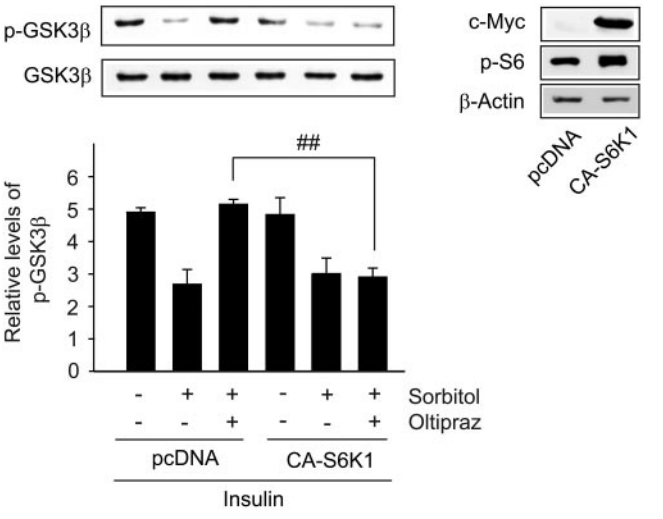

Fig. 5. CA-S6K1 abrogates oltipraz's protection of GSK3β phosphorylation. HepG2 cells transfected with pcDNA or a plasmid encoding CA-S6K1 (1 μg) were treated with 30 μM oltipraz for 1 h, exposed to 600 mM sorbitol for 50 min, and then continuously incubated with 10 nM insulin for 10 min. Data represent mean ± S.E. with at least three separate experiments (##, $p < 0.01$). Immunoblottings for c-Myc and p-S6 verify the expression of CA-S6K1.

praz increased AMPK activity 4 or 8 h after treatment, as assessed by ACC phosphorylation (Fig. 8A, left). However, the extent of S6 phosphorylation was unchanged. In differentiated 3T3-L1 adipocytes that had been incubated in a medium deprived of serum for 12 h, oltipraz treatment only slightly enhanced ACC phosphorylation (i.e., 1–4 h) but failed to decrease S6 phosphorylation (Fig. 8A, right). Because serum starvation alone increased ACC phosphorylations in the cell, the increase in ACC phosphorylation was not distinct 8 h after treatment. These results suggest that oltipraz might not inhibit S6K1 activity in differentiated myotubes or adipocytes despite AMPK activation.

To additionally assess insulin responses in these cells, we determined the functional effects of oltipraz on Akt phosphorylation and glucose uptake in C2C12 myotubes and 3T3-L1 adipocytes. Incubation of the cells with sorbitol completely inhibited insulin-dependent Akt phosphorylation, whereas concomitant oltipraz treatment partly enhanced the insulin-dependent Akt phosphorylation (Fig. 8B, left). Oltipraz was also active in restoring insulin-dependent glucose uptake in sorbitol-treated C2C12 myotubes. In 3T3-L1 adipocytes, sorbitol impairment of insulin-dependent Akt phosphorylation and glucose uptake were not notably or significantly changed by oltipraz treatment (Fig. 8B, right), suggesting that oltipraz restores insulin signals in a cell type-specific manner.

As a continuing effort to confirm the functional effectiveness of the 1,2-dithiole-3-thione compounds, we finally examined glucose uptake into C2C12 myotubes. Among the compounds, CJ11792 or CJ12073 significantly enhanced insulin-dependent glucose uptake into C2C12 myotubes under hyperosmotic stress (Fig. 8C). Taken as a whole, these results demonstrate that treatment with oltipraz or certain 1,2-dithiole-3-thione derivatives allows cells to restore insulin signaling against hyperosmotic stress and thus functionally improves insulin response.

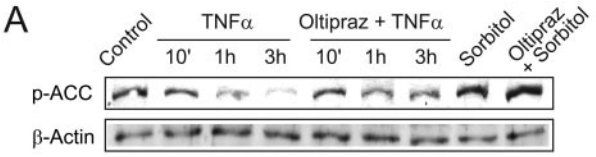

B

Target	Hyperosmolarity		TNFα	
	Oltipraz		Oltipraz	
	−	+	−	+
IRS1-Ser Ⓟ	↑	Inhibition	↑	Inhibition
Akt-Ⓟ	↓	Restoration	↓	Restoration
S6K1-Ⓟ	↑	Inhibition	↑	Inhibition
ACC-Ⓟ	↑	No change	↓	Restoration

Fig. 6. The effect of oltipraz on ACC phosphorylation in TNFα-treated HepG2 cells. A, immunoblotting for ACC phosphorylation. HepG2 cells were treated with 10 ng/ml TNFα for the indicated time period with or without 30 μM oltipraz pretreatment for 1 h and subjected to immunoblot analysis. Results were confirmed by repeated experiments. B, a summary of the effects of oltipraz on HepG2 cells exposed to hyperosmolarity or TNFα. Arrows represent increase or decrease in the level of phosphorylation of target protein.

Discussion

In this study, we found that oltipraz treatment effectively abrogated the IRS1 serine phosphorylation stimulated by hyperosmotic stress elicited by sorbitol, mannitol, or sodium chloride. Oltipraz's inhibition of IRS1 serine phosphorylation led to the recovery of the impaired insulin signaling cascade at the levels of IRS1 tyrosine phosphorylations and Akt/GSK3β phosphorylations. These results are in agreement with our previous findings showing that oltipraz prevented hepatic insulin resistance in mice challenged with endotoxin (or TNFα) or in *lep*$^{ob/ob}$ mice and in mice fed a high-fat diet (Bae et al., 2007). In an additional experiment, we tried to establish an in vivo hyperosmotic shock model. When rats were infused 25% sorbitol solutions for a 10-min period, blood glucose levels increased from 88 to 293 mg/dl at 6 h after the infusion (n = 3, data not shown), which was comparable with the data reported previously (Kaya et al., 2004). However, the liver tissues obtained 10 h after sorbitol infusion exhibited severe injuries. It seemed that the soaring blood glucose

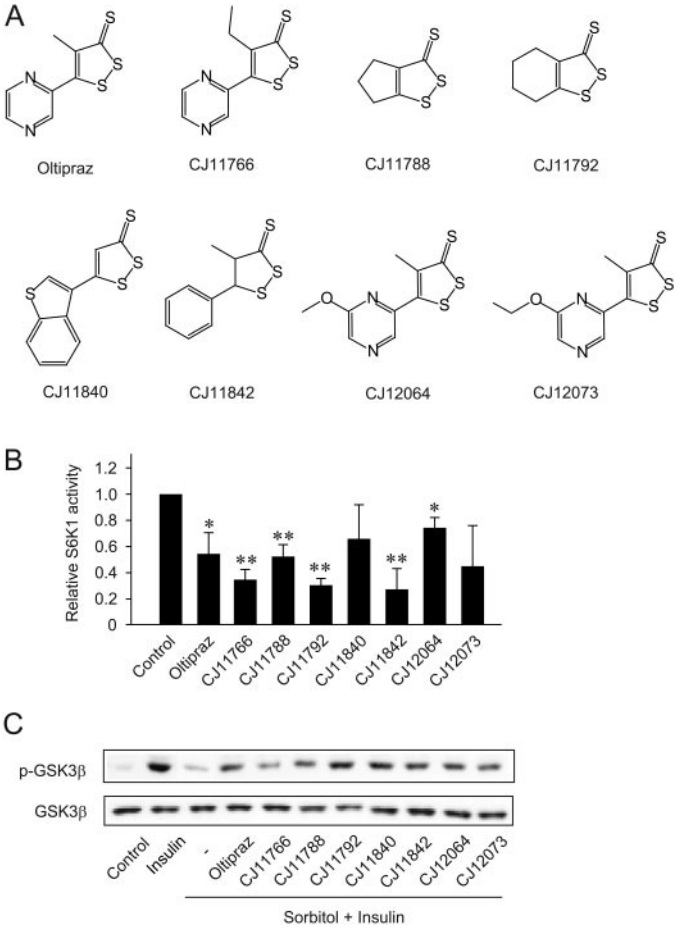

Fig. 7. The compounds containing 1,2-dithiole-3-thione as a pharmacophore inhibit S6K1 activity and thereby protect the ability of insulin to induce GSK3β phosphorylation. A, chemical structures of 1,2-dithiole-3-thione analogs. B, immunocomplex kinase assays for S6K1. S6K1 activity was determined in S6K1 immunoprecipitates prepared from HepG2 cells that had been treated with 30 μM of each 1,2-dithiole-3-thione for 1 h. Data represent mean ± S.E. with at least three separate experiments (*, $p < 0.05$; **, $p < 0.01$, significant compared with vehicle-treated control; control level = 1). C, GSK3β phosphorylations. The cells were treated with 30 μM dithiolethione derivative for 1 h, exposed to 600 mM sorbitol for 50 min, and then continuously incubated with 10 nM insulin for 10 min. Phosphorylated GSK3β was immunoblotted in cell lysates.

contents may have resulted from strong activation of sympathetic nervous system and/or severe liver damage. In clinical situations, hyperosmotic hyperglycemic state is manifested by serum osmolarity greater than 320 mOsM and blood glucose levels greater than 600 mg/dl (Kitabchi et al., 2004), with a dramatic increase in the prevalence of type 2 diabetes (Ennis et al., 1994). Although the hyperosmolarity induced by 600 mM sorbitol in the present cell culture study is not attainable in a physiological state, our experimental results are worthy of understanding the molecular mechanism of hyperosmotic insulin resistance.

In the present study, we observed that hyperosmolarity causes S6K1 activation in HepG2 cells, which was evidenced by increases in both S6K1 immune-complex kinase activity and S6 phosphorylation. It has been reported that a high concentration of sorbitol elicits IRS1 dysfunction by an mTOR-dependent pathway (Gual et al., 2003a). Because mTOR targets S6K1, it could be expected that the conditions of hyperosmotic stress led to S6K1 activation. Chen et al. have shown that hyperosmotic stress increased the basal S6K1 activity ~3-fold in 3T3-L1 adipocytes (Chen et al., 1999). However, it was also claimed that hyperosmolarity inhibited the basal S6K1 activity in CV1 and Jurkat cells (Parrott and Templeton, 1999; Fumarola et al., 2005), and insulin-dependent S6K1 activation in 3T3-L1 adipocytes or H4IIE cells (Chen et al., 1999; Lornejad-Schäfer et al., 2003). Despite the reported cell type-specific controversial effects of hyperosmolarity on S6K1, our results lend support to the concept that the mTOR-dependent IRS1 serine phosphorylation results from S6K1 activation.

mTOR, once activated, phosphorylates and activates S6K1, which then increases S6 phosphorylations. As expected, S6 phosphorylations enhanced by hyperosmotic stress were completely abrogated by oltipraz pretreatment. In addition, phosphorylation of 4E-BP1, an alternative direct target of mTOR, could be inhibited by oltipraz. The principal finding of this study therefore relates to the inhibitory effect of oltipraz on hyperosmotic S6K1 activation, and this observation is strengthened by the result of our DN-S6K1 experiment. These observations lend support to the notion that oltipraz

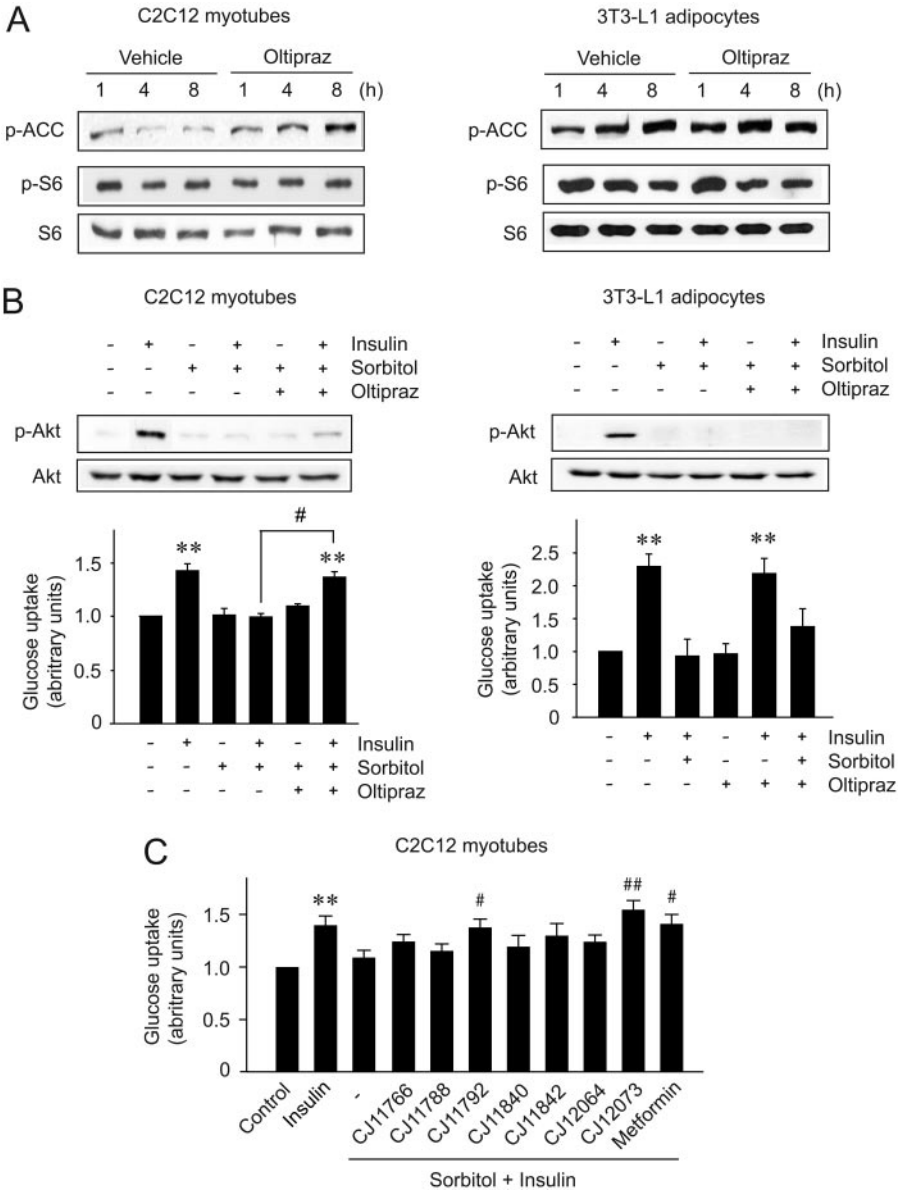

Fig. 8. Oltipraz or other 1,2-dithiole-3-thione derivatives functionally improve insulin responses against hyperosmotic stress in C2C12 myotubes. A, the effect of oltipraz on the phosphorylations of ACC and S6. Immunoblot analysis was performed in cell lysates obtained from C2C12 myotubes (left) or 3T3-L1 adipocytes (right) treated with vehicle or 30 μM oltipraz for the indicated time period. B, insulin-dependent Akt phosphorylation (Ser^{473}) and glucose uptake in C2C12 myotubes (left) and in 3T3-L1 adipocytes (right). Myotubes or adipocytes were treated with 30 μM oltipraz for 1 h, exposed to 600 mM sorbitol for 50 min, and then continuously incubated with 10 nM insulin for 10 min. Akt phosphorylations were determined in cell lysates. Glucose uptake was measured in cells treated with 100 nM insulin for 10 min after sorbitol treatment with or without oltipraz pretreatment (1 h). Data represent mean ± S.E. with at least 4 separate experiments (**, $p < 0.01$, significant compared with vehicle control; #, $p < 0.05$, significant compared with sorbitol + insulin). C, glucose uptake in C2C12 myotubes treated with 30 μM concentrations of each compound. Metformin (1 mM, 1 h) was used as a positive control. Data represent mean ± S.E. with at least four separate experiments (**, $p < 0.01$, significant compared with vehicle control; #, $p < 0.05$; ##, $p < 0.01$, significant compared with sorbitol + insulin).

selectively affects S6K1 activity probably through inhibition of the mTOR pathway. Our current finding that JNK1/2, ERK1/2, p38 MAPK, and nuclear factor-κB pathways activated by hyperosmotic stress were unchanged by oltipraz supports the relatively specific inhibition of oltipraz on hyperosmotic activation of S6K1. Oltipraz's inhibition of S6K1 led to the recovery of the impaired insulin signaling cascade at the level of IRS1 tyrosine phosphorylation and Akt and GSK3β phosphorylations. Moreover, in this work, CA-S6K1 transfection abrogated the ability of oltipraz to restore GSK3β phosphorylation, verifying the functional significance of S6K1 inhibition by oltipraz in improving insulin signals. Our data corroborating the selective S6K1 inhibition by oltipraz among sorbitol-activated kinases in conjunction with the causal relationship between S6K1 inhibition and improved insulin responses provide strong evidence that oltipraz's restoration of insulin sensitivity against hyperosmotic stress results from S6K1 inhibition.

The principal glucose transporter protein that mediates glucose uptake into skeletal muscle is GLUT4, which plays a key role in regulating whole body glucose homeostasis. In response to insulin, Akt and other signaling molecules, such as atypical protein kinase C λ/ζ, AMPK, calcium/calmodulin-dependent protein kinase II, and classic protein kinase C regulate GLUT4 trafficking (Farese et al., 2005; Jessen and Goodyear, 2005; Rose and Richter, 2005). The beneficial effects of oltipraz on the functional improvement in insulin actions are supported by the observations demonstrating that insulin-dependent glucose uptake inhibited by hyperosmotic stress in C2C12 myotubes was significantly restored by oltipraz. These results are consistent with the finding that oltipraz also protected insulin-dependent Akt phosphorylation. However, oltipraz failed to recover Akt phosphorylation and glucose uptake in sorbitol-treated 3T3-L1 adipocytes. In separate experiments, we found that rapamycin, a potent inhibitor of mTOR-S6K1 pathway, prevented insulin resistance in HepG2 or H4IIE cells (evidenced by increases in Akt phosphorylation), but not in 3T3-L1 adipocytes even at the concentration that perfectly inhibited S6 phosphorylations (data not shown). From the above results, it could be speculated that pathway(s) alternative to the mTOR-S6K pathway function(s) in adipocytes exposed to hyperosmolarity.

Furthermore, we demonstrated that a variety of synthetic 1,2-dithiole-3-thione compounds strongly inhibited S6K1 activity, indicating that the active moiety capable of exerting S6K1 inhibition exists in the 1,2-dithiole-3-thione moiety. S6K1 inhibition by the compounds comprising 1,2-dithiole-3-thione as a pharmacophore contributed to the improvement of insulin signaling, as evidenced by increases in GSK3β phosphorylation against hyperosmotic stress. This concurs with our previous finding that the 1,2-dithiole-3-thiones also enhanced insulin responses from TNFα-induced impairment (Bae et al., 2007). In the present study, the extent of S6K1 inhibition by the compounds did not completely match with that of either GSK3β phosphorylation or glucose uptake, which might be due to the limit of sensitivity of the kinase assay or intricate regulatory mechanism underlying glucose uptake into muscle cells. Our contention is supported by the results showing that the synthetic dithiolethiones consistently decreased S6 phosphorylation in either HepG2 (data not shown) or H4IIE cells (Bae et al., 2007). Despite the variability in their efficacies, some of the 1,2-dithiole-3-thiones (i.e., 4,5,6,7-tetrahydrobenzo-1,2-dithiole-3-thione (CJ11792) and 5-(6-ethoxypyrazin-2-yl)-4-methyl-1,2-dithiole-3-thione (CJ12073)) significantly increased insulin-dependent glucose uptake impaired by hyperosmotic stress in C2C12 myotubes. Complete dose response, and pharmacodynamic and pharmacokinetic studies of these candidates remain to be established in the future.

We have shown that oltipraz and other dithiolethiones activate AMPK and that their AMPK-dependent S6K1 inhibition plays a key role in abolishing TNFα-induced insulin resistance (Bae et al., 2007). Here, in this study, hyperosmotic conditions activated both mTOR-S6K1 and AMPK. The results of energy depletion and gene knockout experiments showed that AMPK activation leads to suppression of the mTOR pathway via phosphorylation of tuberous sclerosis complex 2, a negative regulator of mTOR-S6K1 (Krause et al., 2002; Inoki et al., 2003; Brugarolas et al., 2004; Shaw et al., 2004). It seems likely that hyperosmotic stress activates S6K1 irrespectively of its AMPK activation. In the present study, we observed that TNFα decreased AMPK activity in HepG2 cells, which is consistent with the result showing that TNFα inhibited AMPK via transcriptional up-regulation of PP2C (Steinberg et al., 2006), supporting the concepts that S6K1 activation by TNFα involves alteration in AMPK activity and that the inhibitory effect of oltipraz on TNFα-induced S6K1 activation depends on AMPK activation (Bae et al., 2007). Our results and others indicate that the pathway responsible for mTOR-S6K1 activation by hyperosmolarity may differ from that by TNFα. Our observation also showed that sorbitol treatment markedly increased ACC phosphorylation without altering cellular ATP content (data not shown). In general, hyperosmotic AMPK activation is associated with a decrease in cellular generation of ATP, phosphocreatine, and glycogen (Hayashi et al., 1998, 2000), suggesting that the activation of AMPK by hyperosmolarity results from adaptive response to toxic stimuli. Therefore, it could be concluded that the signaling pathway of AMPK activation by oltipraz differs from that by hyperosmolarity. Our observations showing that the prevention of hyperosmotic insulin resistance results from the inhibition of S6K1 indicate that 1,2-dithiole-3-thiones inhibit S6K1 activation independently of the hyperosmotic stress-induced AMPK activation. This hypothesis is in fact supported by our additional data showing that DN-AMPK transfection failed to reverse the ability of oltipraz to restore insulin sensitivity in cells treated with 600 mM sorbitol for 1 h (data not shown).

In conclusion, the results presented in this study demonstrate that the compounds comprising 1,2-dithiole-3-thione as a pharmacophore improved insulin sensitivity under the condition of hyperosmotic stress, which resulted from the inhibition of S6K1 activation. Moreover, this study revealed that S6K1 downstream of mTOR was responsible for hyperosmotic stress-induced insulin resistance. The current study brings additional insights into the therapeutic effects of 1,2-dithiole-3-thione compounds on insulin resistance, which may be of assistance in developing drugs to treat insulin resistance.

References

Aguirre V, Uchida T, Yenush L, Davis R, and White MF (2000) The c-Jun NH_2-terminal kinase promotes insulin resistance during association with insulin receptor substrate-1 and phosphorylation of Ser(307). *J Biol Chem* **275:**9047–9054.

Aguirre V, Werner ED, Giraud J, Lee YH, Shoelson SE, and White MF (2002) Phosphorylation of Ser307 in insulin receptor substrate-1 blocks interactions with the insulin receptor and inhibits insulin action. *J Biol Chem* **277:**1531–1537.

Bae EJ and Kim SG (2005) Enhanced CCAAT/enhancer-binding protein beta-liver-enriched inhibitory protein production by oltipraz, which accompanies CUG repeat-binding protein-1 (CUGBP1) RNA-binding protein activation, leads to inhibition of preadipocyte differentiation. *Mol Pharmacol* **68:**660–669.
Bae EJ, Yang YM, Kim JW, and Kim SG (2007) Identification of a novel class of dithiolethiones that prevent hepatic insulin resistance via adenosine monophosphate activated protein kinase-p70S6 kinase 1 pathway. *Hepatology* **46:**730–739.
Bratusch-Marrain PR, and DeFronzo RA (1983) Impairment of insulin-mediated glucose metabolism by hyperosmolality in man. *Diabetes* **32:**1028–1034.
Brugarolas J, Lei K, Hurley RL, Manning BD, Reiling JH, Hafen E, Witters LA, Ellisen LW, and Kaelin WG Jr (2004) Regulation of mTOR function in response to hypoxia by REDD1 and the TSC1/TSC2 tumor suppressor complex. *Genes Dev* **18:**2893–2904.
Chen D, Fucini RV, Olson AL, Hemmings BA, and Pessin JE (1999) Osmotic shock inhibits insulin signaling by maintaining Akt/protein kinase B in an inactive dephosphorylated state. *Mol Cell Biol* **19:**4684–4694.
Curphey TJ (2002) Thionation with the reagent combination of phosphorus pentasulfide and hexamethyldisiloxane. *J Org Chem* **67:**6461–6473.
Eisner V, Quiroga C, Criollo A, Eltit JM, Chiong M, Parra V, Hidalgo K, Toro B, and Díaz-Araya G, Lavandero S (2006) Hyperosmotic stress activates p65/RelB NFkappaB in cultured cardiomyocytes with dichotomic actions on caspase activation and cell death. *FEBS Lett* **580:**3469–3476.
Engelman JA, Berg AH, Lewis RY, Lisanti MP, and Scherer PE (2000) Tumor necrosis factor alpha-mediated insulin resistance, but not dedifferentiation, is abrogated by MEK1/2 inhibitors in 3T3–L1 adipocytes. *Mol Endocrinol* **14:**1557–1569.
Ennis ED, Stahl E, and Kreisberg RA (1994) The hyperosmolar hyperglycemic syndrome. *Diabetes Rev* **2:**115–126.
Farese RV, Sajan MP, and Standaert ML (2005) Insulin-sensitive protein kinases (atypical protein kinase C and protein kinase B/Akt): actions and defects in obesity and type II diabetes. *Exp Biol Med* **230:**593–605.
Fryer LG, Hajduch E, Rencurel F, Salt IP, Hundal HS, Hardie DG, and Carling D (2000) Activation of glucose transport by AMP-activated protein kinase via stimulation of nitric oxide synthase. *Diabetes* **49:**1978–1985.
Fumarola C, La Monica S, and Guidotti GG (2005) Amino acid signaling through the mammalian target of rapamycin (mTOR) pathway: role of glutamine and of cell shrinkage. *J Cell Physiol* **204:**155–165.
Galcheva-Gargova Z, Dérijard B, Wu IH, and Davis RJ (1994) An osmosensing signal transduction pathway in mammalian cells. *Science* **265:**806–808.
Galvez AS, Ulloa JA, Chiong M, Criollo A, Eisner V, Barros LF, and Lavandero S (2003) Aldose reductase induced by hyperosmotic stress mediates cardiomyocyte apoptosis: differential effects of sorbitol and mannitol. *J Biol Chem* **278:**38484–38494.
Gao Z, Hwang D, Bataille F, Lefevre M, York D, Quon MJ, and Ye J (2002) Serine phosphorylation of insulin receptor substrate 1 by inhibitor κB kinase complex. *J Biol Chem* **277:**48115–48121.
Gual P, Gonzalez T, Gremeaux T, Barres R, Le Marchand-Brustel Y, and Tanti JF (2003a) Hyperosmotic stress inhibits insulin receptor substrate-1 function by distinct mechanisms in 3T3–L1 adipocytes. *J Biol Chem* **278:**26550–26557.
Gual P, Le Marchand-Brustel Y, and Tanti JF (2003b) Positive and negative regulation of glucose uptake by hyperosmotic stress. *Diabetes Metab* **29:**566–575.
Han J, Lee JD, Bibbs L, and Ulevitch RJ (1994) A MAP kinase targeted by endotoxin and hyperosmolarity in mammalian cells. *Science* **265:**808–811.
Harrington LS, Findlay GM, Gray A, Tolkacheva T, Wigfield S, Rebholz H, Barnett J, Leslie NR, Cheng S, Shepherd PR, et al. (2004) The TSC1–2 tumor suppressor controls insulin-PI3K signaling via regulation of IRS proteins. *J Cell Biol* **166:**213–223.
Hayashi T, Hirshman MF, Fugii N, Habinowski SA, Witters LA, and Goodyear LJ (2000) Metabolic stress and altered glucose transport. Activation of AMP-activated protein kinase as a unifying coupling mechanism. *Diabetes* **49:**527–531.
Hayashi T, Hirshman MF, Kurth EJ, Winder WW, and Goodyear LJ (1998) Evidence for 5′ AMP-activated protein kinase mediation of the effect of muscle contraction on glucose transport. *Diabetes* **47:**1369–1373.
Hotamisligil GS, Peraldi P, Budavari A, Ellis R, White MF, and Spiegelman BM (1996) IRS-1-mediated inhibition of insulin receptor tyrosine kinase activity in TNF-alpha- and obesity-induced insulin resistance. *Science* **271:**665–668.
Inoki K, Zhu T, and Guan KL (2003) TSC2 mediates cellular energy response to control cell growth and survival. *Cell* **115:**577–590.
Jefferies HB, Fumagalli S, Dennis PB, Reinhard C, Pearson RB, and Thomas G (1997) Rapamycin suppresses 5′TOP mRNA translation through inhibition of p70s6k. *EMBO J* **16:**3693–3704.
Jessen N and Goodyear LJ (2005) Contraction signaling to glucose transport in skeletal muscle. *J Appl Physiol* **99:**330–337.
Kang KW, Cho IJ, Lee CH, and Kim SG (2003) Essential role of phosphatidylinositol 3-kinase-dependent CCAAT/enhancer binding protein beta activation in the induction of glutathione S-transferase by oltipraz. *J Natl Cancer Inst* **95:**53–66.
Kaya M, Gulturk S, Elmas I, Kalayci R, Arican N, Kocyildiz ZC, Kucuk M, Yorulmaz H, and Sivas A (2004) The effects of magnesium sulfate on blood-brain barrier disruption caused by intracarotid injection of hyperosmolar mannitol in rats. *Life Sci* **76:**201–212.
Kayali AG, Austin DA, and Webster NJ (2000) Stimulation of MAPK cascades by insulin and osmotic shock: lack of an involvement of p38 mitogen-activated protein kinase in glucose transport in 3T3–L1 adipocytes. *Diabetes* **49:**1783–1793.
Kitabchi AE, Umpierrez GE, Murphy MB, Barrett EJ, Kreisberg RA, Malone JI, and Wall BM; American Diabetes Association (2004) Hyperglycemic crises in diabetes. *Diabetes Care* **27 (Suppl 1):**S94–S102.
Krause U, Bertrand L, and Hue L (2002) Control of p70 ribosomal protein S6 kinase and acetyl-CoA carboxylase by AMP-activated protein kinase and protein phosphatases in isolated hepatocytes. *Eur J Biochem* **269:**3751–3759.
Kültz D, Garcia-Perez A, Ferraris JD, and Burg MB (1997) Distinct regulation of osmoprotective genes in yeast and mammals. Aldose reductase osmotic response element is induced independent of p38 and stress-activated protein kinase/Jun N-terminal kinase in rabbit kidney cells. *J Biol Chem* **272:**13165–13170.
Lornejad-Schäfer MR, Schafer C, Graf D, Haussinger D, and Schliess F (2003) Osmotic regulation of insulin-induced mitogen-activated protein kinase phosphatase (MKP-1) expression in H4IIE rat hepatoma cells. *Biochem J* **371:**609–619.
Myers MG Jr and White MF (1996) Insulin signal transduction and the IRS proteins. *Annu Rev Pharmacol Toxicol* **36:**615–658.
Parrott LA and Templeton DJ (1999) Osmotic stress inhibits p70/85 S6 kinase through activation of a protein phosphatase. *J Biol Chem* **274:**24731–24736.
Paz K, Voliovitch H, Hadari YR, Roberts CT Jr., LeRoith D, and Zick Y (1996) Interaction between the insulin receptor and its downstream effectors. Use of individually expressed receptor domains for structure/function analysis. *J Biol Chem* **271:**6998–7003.
Pearson RB, Dennis PB, Han JW, Williamson NA, Kozma SC, Wettenhall RE, and Thomas G (1995) The principal target of rapamycin-induced p70s6k inactivation is a novel phosphorylation site within a conserved hydrophobic domain. *EMBO J* **14:**5279–5287.
Rose AJ and Richter EA (2005) Skeletal muscle glucose uptake during exercise: how is it regulated? *Physiology* **20:**260–270.
Saltiel AR and Kahn CR (2001) Insulin signaling and the regulation of glucose and lipid metabolism. *Nature* **414:**799–806.
Shaw RJ, Bardeesy N, Manning BD, Lopez L, Kosmatka M, DePinho RA, and Cantley LC (2004) The LKB1 tumor suppressor negatively regulates mTOR signaling. *Cancer Cell* **6:**91–99.
Steinberg GR, Carling D, Hotamisligil GS, Febbraio MA, Kay TW, and Kemp BE (2006) Tumor necrosis factor alpha-induced skeletal muscle insulin resistance involves suppression of AMP-kinase signaling. *Cell Metab* **4:**465–474.
Sun XJ, Goldberg JL, Qiao LY, and Mitchell JJ (1999) Insulin-induced insulin receptor substrate-1 degradation is mediated by the proteasome degradation pathway. *Diabetes* **48:**1359–1364.
Tremblay F, Krebs M, Dombrowski L, Brehm A, Bernroider E, Roth E, Nowotny P, Waldhausl W, Marette A, and Roden M (2005) Overactivation of S6 kinase 1 as a cause of human insulin resistance during increased amino acid availability. *Diabetes* **54:**2674–2684.
Um SH, Frigerio F, Watanabe M, Picard F, Joaquin M, Sticker M, Fumagalli S, Allegrini PR, Kozma SC, Auwerx J, et al. (2004) Absence of S6K1 protects against age- and diet-induced obesity while enhancing insulin sensitivity. *Nature* **431:**200–205.
Yamauchi T, Tobe K, Tamemoto H, Ueki K, Kaburagi Y, Yamamoto-Honda R, Takahashi Y, Yoshizawa F, Aizawa S, Akanuma Y, et al. (1996) Insulin signalling and insulin actions in the muscles and livers of insulin-resistant, insulin receptor substrate 1-deficient mice. *Mol Cell Biol* **16:**3074–3084.

Address correspondence to: Sang Geon Kim, Ph.D., College of Pharmacy, Seoul National University, Sillim-dong, Kwanak-gu, Seoul 151-742, Korea. E-mail: sgk@snu.ac.kr